Proceedings of the 3rd IFAC Workshop on
Thermodynamic Foundations for a Mathematical Systems
Theory, Louvain-la-Neuve, Belgium, July 3-5, 2019

Modelling of thermo–acoustic instabilities

Benjamin Vincent [*,**] **Nicolas Hudon** [***] **Laurent Lefèvre** [**]
Denis Dochain [*]

[*] *ICTEAM, Université Catholique de Louvain, Bâtiment Euler, av. Lemaître 4-6, B-1348 Louvain-La-Neuve, Belgium. (e-mail:{benjamin.vincent,denis.dochain}@uclouvain.be)*
[**] *Univ. Grenoble Alpes, Grenoble INP, LCIS, 26000 Valence, France (e-mail:laurent.lefevre@lcis.grenoble-inp.fr)*
[***] *Department of Chemical Engineering, Queen's University, Kingston, ON, K7L 3N6 Canada. (e-mail:nicolas.hudon@queensu.ca)*

Abstract: This paper proposes a combination of mixed finite and infinite port–Hamiltonian (m–phs) control models describing thermo–acoustic instabilities in Rijke's tubes. This experimental setup is a vertical tube open at both ends where a heating element is embedded at its lower part. Thermo–acoustic instabilities occur when the heat transfer is coupled with the acoustic field and generates a loud humming sound. Instabilities can be rejected with a boundary feedback controller. The acoustic pressure at the tube's top end is measured while the acoustic velocity is actuated at the bottom of the tube with a loudspeaker. The loudspeaker, the heat release process, and the open–end impedance are governed by finite–dimensional port–Hamiltonian systems. The acoustic field is represented as interconnected wave equations. All subsystems are interconnected through power preserving structures enabling the formulation of the open loop as a m–phs.

Keywords: Thermo-acoustics instabilities, Port-Hamiltonian systems, Boundary control systems, Rijke's tube, Multi–physics systems

1. INTRODUCTION

The Rijke tube experiment consists of a vertical tube, open at both ends, where an internal heat source is embedded at its first lower part (see Figure 1). This is used in laboratory to illustrate and study thermo–acoustics phenomena appearing in a large range of real–life applications, *e.g.* gas turbines, columns, combustion processes, etc. (Annaswamy and Ghoniem, 2002). The instability occurs when heat transfer and acoustics dynamics are coupled and manifest itself with the production of a loud humming sound which natural frequency is the one of the open tube. The fundamental wavelength of the Rijke tube is twice the tube length and higher harmonics are multiple integers of this frequency. The heating element generates a natural convection due to the buoyancy of air. Small perturbations on the heating area travel within the tube, reflect at its boundary, turn over and disturb the heat release process again and a sustained periodic acoustic phenomena is generated (Rayleigh, 1878).

Thermo–acoustic phenomena, and more generally combustion instabilities, are modelled by partial differential equations: the Euler equations which is obtained from continuity equation, and momentum and internal energy balance equations. The air within the tube is subject to gravitational forces and the heating element is a local internal energy source term. The model reduces to a wave–like equation on which a separation of variables can be applied to derive a set of ordinary differential equations, defining the harmonics dynamics (Culick and Kuentzmann, 2006). A finite–dimensional model–based control approach was investigated with phase shift (Heckl, 1988), proportional integral (Fung and Yang, 1992), adaptive (Krstic et al., 1999), and robust controllers (Jacobson et al., 2000; Chu et al., 2003), and (Dowling and Morgans, 2005).

The thermo–acoustic instability control problem resurfaced in recent studies as an infinite–dimensional control problem (Epperlein et al., 2015). The wave equation, reformulated in characteristic coordinates, enable the development of backstepping boundary control and state estimator design (de Andrade et al., 2018b,a).

In this contribution, we propose a geometric model of the thermo–acoustic phenomena. The port–Hamiltonian formulation relies on a physics-based modelling approach which is recognized as valuable when treating multi–physics systems (Duindam et al., 2009). A combination of mixed finite and infinite port–Hamiltonian system (m–phs) is derived to model the Rijke tube. Notably, the locally distributed heat source, usually modelled with a Dirac structure, is here replaced by an energy–preserving interconnection coupling two wave equations and a nonlinear model of the heat release process. The spatial domain is decomposed in two parts, each of them being governed by a linear wave equation interconnected to the heat release element, a finite dimensional system. Furthermore the top–end acoustic impedance of the tube (Zimmer et al., 2003) and the loudspeaker (Falaize et al., 2015) dynamics are governed by linear ordinary differential equations, re–formulated as linear port–Hamiltonian systems.

[1] The first author is a FRIA fellow (F.R.S.-FNRS).

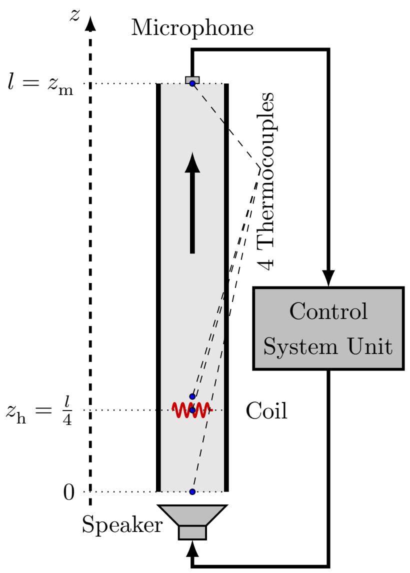

Fig. 1. Schematic of the experimental Rijke tube setup

The paper is structured as follows. Section 2 presents the Rijke tube experiment and the class boundary control port–Hamiltonian systems. In Section 3 a first–principle nonlinear fluid–like model of the Rijke Tube is introduced. In Section 4 all sub–systems are formulated within the port–Hamiltonian framework. The complete m–phs of the Rijke tube is derived in Section 5. Conclusions and future areas for investigations based on the proposed model formulation are discussed in Section 6.

2. BACKGROUND

2.1 Experimental Rijke's tube

The experimental Rijke's tube built at UCLouvain possess the following dimensions: length $l = 1.5\,m$, internal diameter $d = 7.3\,cm$ (radius a), with a nichrome coil of diameter $6\,mm$ of linear impedance $1.73\,\Omega m^{-1}$. An external power supply (*Elektro-Automatik PSI 5080-20A*) is set in current mode to apply a constant current $I_{\mathrm{w}} = 11.5\,A$ which provides a total power of $205\,W$. The control law can be implemented in the micro–controller/FPGA real-time target (*NI myRIO 1950*) connected to a computer running an interface (*Labview*) for data recording and supervision. A loudspeaker (*Visaton FR 12–8Ω*) is place at the bottom of the tube and is used as a boundary actuator. We have experienced troubles to find an appropriate coil geometry able to trigger the thermo-acoustic instability. As a result we concluded that a high amount of released power does not necessarily trigger the instability. One has to be sure to generate a large gradient in temperature over a small volume around the heating element. Therefore we have designed a 3 wire parallel heater, each coil made of a $1\,m$ long wire with winding diameter $0.5\,cm$.

2.2 Boundary port–Hamiltonian systems

We consider the class of infinite–dimensional boundary port–Hamiltonian systems, which takes the following form (Jacob and Zwart, 2012)

$$\frac{\partial x}{\partial t}(t,z) = P_1 \frac{\partial}{\partial z}\left(\mathcal{L}(z)x(t,z)\right) + P_0\mathcal{L}(z)x(t,z), \quad (1)$$

with $z \in [a,b]$, the spatial variable, and $t \in [0,+\infty)$, the time variable. The matrix $P_1 \in M_n(\mathbb{R})$ is a square n dimensional non–singular symmetric matrix and $P_0 = -P_0^\top \in M_n(\mathbb{R})$. The state variable x takes value in $\mathbb{R}^n$. Furthermore, the matrix-valued function $\mathcal{L}(z) \in L_\infty([a,b], M_n(\mathbb{R}))$ is bounded. The system is defined with the following pairs of boundary variables:

$$\begin{pmatrix} f_\partial \\ e_\partial \end{pmatrix} = \frac{1}{\sqrt{2}} \begin{pmatrix} P_1 & -P_1 \\ I_n & I_n \end{pmatrix} \begin{pmatrix} \mathcal{L}(z)x(t,a) \\ \mathcal{L}(z)x(t,b) \end{pmatrix}. \quad (2)$$

Boundary conditions, inputs, and outputs are defined with matrices $W_{b,1}$, $W_{b,2}$, and W_c of appropriate size and such that

$$\begin{pmatrix} u(t) \\ 0 \\ y(t) \end{pmatrix} = \begin{pmatrix} W_{B,1} \\ W_{B,2} \\ W_C \end{pmatrix} \begin{pmatrix} f_\partial \\ e_\partial \end{pmatrix}. \quad (3)$$

Existence and uniqueness of a solution for the above PDE follows from semi–group theory (Jacob and Zwart, 2012). The state space is labelled $\mathcal{X}$, a Hilbert space, $\mathcal{X} = L_2([a,b];\mathbb{R}^n)$, the space of measurable square–integrable real–valued functions, equipped with the inner product $\langle\cdot,\cdot\rangle$ and the norm $\|\cdot\| = \sqrt{\langle\cdot,\cdot\rangle}$. The control input u satisfies $u \in C^2([0,+\infty);\mathbb{R}^n)$. The Sobolev space of order p is denoted $H^p([a,b];\mathbb{R}^p)$.

The homogeneous port–Hamiltonian system defines an operator given by an unbounded operator

$$Ax = P_1 \frac{d}{dz}(\mathcal{L}x) + P_0\mathcal{L}x, \quad (4)$$

with the domain

$$D(A) = \left\{ \mathcal{L}x \in H^1\left((a,b);\mathcal{R}^n\right) \,\middle|\, \begin{pmatrix} (\mathcal{L}x)(b) \\ (\mathcal{L}x)(a) \end{pmatrix} \in \ker W_B \right\},$$

where $W_B^\top = \begin{pmatrix} W_{B,1}^\top & W_{B,1}^\top \end{pmatrix}$. In this contribution, we consider the following Assumption.

Assumption 1. For the operator (4), associated with PDE (1) with boundary conditions (3), the following assumptions hold:

- The matrix W_B is a $n \times 2n$ full rank matrix;
- For $x_0 \in D(A)$, we have $\langle Ax_0, x_0\rangle \leq 0$.

From assumption 1, it follows (see Jacob and Zwart (2012)) that the state equation (1) with boundary conditions (3) is a boundary control system, and for $u \in C^2\left([0,+\infty);\mathbb{R}^k\right)$, and $\mathcal{L}x(0) \in H^1\left((a,b);\mathbb{R}^n\right)$, satisfying the boundary conditions (3), where $k \in \mathbb{N}^+$ is the number of inputs, there exists a unique classical solution for the system (1)–(3).

3. RIJKE'S TUBE MODELLING

The Rijke tube dynamics are described by the following set of balance equations (mass, momentum, energies):

$$\frac{\partial \rho}{\partial t} + \frac{\partial}{\partial z}(\rho v) = 0 \quad (5)$$

$$\frac{\partial \rho v}{\partial t} + \frac{\partial}{\partial z}\left(\frac{1}{2}\rho v^2 + p\right) = -\rho g \quad (6)$$

$$\frac{\partial \rho e}{\partial t} + \frac{\partial}{\partial z}\left(\rho v e + v p + j_q\right) = \rho q - \rho g \quad (7)$$

$$\frac{\partial \rho u}{\partial t} + \frac{\partial}{\partial z}\left(\rho v u + j_q\right) = -p\frac{\partial v}{\partial z} + \rho q, \quad (8)$$

where $t \in [0,+\infty)$ and $z \in [0,l]$ denote the time and the spatial variables, respectively. State variables $\rho(t,z)$, $v(t,z)$, and $u(t, z)$ denote the air density, the air velocity, and the air internal energy profiles along the tube. Distributed profiles are measurable square integrable functions, $L_2([0, l])$, equipped with the inner product $\langle \cdot, \cdot \rangle$ and the norm $\| \cdot \| = \sqrt{\langle \cdot, \cdot \rangle}$. The following closure relations are used.

- The total energy profile is the sum of the kinetic and the internal energy, as: $e = \frac{1}{2}v^2 + u$.
- The heat flux, denoted j_q, is defined from Fourier's law, $j_q = \lambda \frac{\partial}{\partial z}\left(\frac{1}{T}\right)$, where λ denote the air heat diffusion coefficient and $T(t, z)$ is the temperature.
- The ideal gas law is assumed, *i.e.*, $\rho u = (C_v/R)p$, where C_v, $p = p(t, z)$, and R denote the specific heat capacity at constant volume, the pressure profile, and the ideal gas constant, respectively.
- The generalized force is represented by the gravitational acceleration g.
- The heat release term $q(t, z)$ is located at $z = z_{\mathrm{h}}$.

Finally the system is initialized with the following data: $\rho(0, z) = \rho_0$, $T(0, z) = T_0$, $v(0, z) = 0$ and is subject to the following boundary conditions: $\rho(t, 0) = \rho_0$, $T(t, 0) = T_0$, $\partial T(t, l)/\partial z = 0$, and $dv(t, 0)/dt = 0$.

Various formulations of the heat release term q exists. The heat transfer between a hot wire and a fluid in motion is characterized by Kings' law. This anemometer model provide a nonlinear formulation (Heckl, 1988), reducing to a first order differential equation with delay (Epperlein et al., 2015). The boundary layer model is sensitive to two parameters representing the heat release time constant and the wire temperature.

An alternative approach to model the Rijke tube consists of interpreting the boundary layer dynamics as a self-sustained oscillator. A van der Pol oscillator provides a good dynamical approximation of the first acoustic mode (Culick and Kuentzmann, 2006; Noiray and Schuermans, 2013). Indeed, this oscillator presents bifurcations, a stable null equilibrium, and self-sustained cycle. All of those dynamical properties are experimentally observed in combustion systems presenting instabilities (Annaswamy and Ghoniem, 2002).

3.1 Disturbed wave equation

We define steady state variables $\overline{\rho}(z) = \rho_0$, $\overline{v}(z)$, and $\overline{p}_0(z)$ as the solution to equations (5)–(8), we introduce the following deviation variables $\widetilde{\rho}(t, z)$, $\widetilde{p}(t, z)$, and $\widetilde{v}(t, z)$. It is assumed that the heat diffusion process is negligible in comparison to the internal energy convection term in the internal energy balance equation (8). The gas dynamics reduces to the following set of two balance equations (Epperlein et al., 2015)

$$\begin{aligned} &\frac{\partial \widetilde{v}}{\partial t}(t, z) + \frac{1}{\overline{\rho}}\frac{\partial \widetilde{p}}{\partial z}(t, z) = 0, \\ &\frac{\partial \widetilde{p}}{\partial t}(t, z) + \gamma \overline{p}\frac{\partial \widetilde{v}}{\partial z}(t, z) = \frac{\overline{\gamma}}{A}\widetilde{q}(t)\delta(z - z_{\mathrm{h}}), \end{aligned} \tag{9}$$

where A, $\overline{\gamma} = \gamma - 1$, and $\widetilde{q}(t)$ represents the tube cross-section, the corrected adiabatic ratio, and the fluctuating heat released per unit volume, respectively. The delta Dirac distribution $\delta(z - z_{\mathrm{h}})$ is centered at position z_{h}. Parameter of this sub–domain are gathered in Table 1. The open top–end of the tube is subject to the following boundary condition:

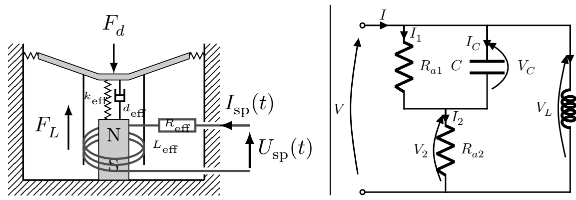

Fig. 2. Schematic of: the loudspeaker (left) — the acoustic end–impedance (right)

$$\widetilde{p}(t, l) = Z_l \widetilde{v}(t, l), \tag{10}$$

where Z_l denotes the specific acoustic impedance at coordinate $z = l$. This impedance can be experimentally measured, or alternatively approximated with an electric circuit analogy (Zimmer et al., 2003). The lower part of the tube is connected to a loudspeaker which dynamics are governed by a mass spring system. Following Zimmer et al. (2003) the loudspeaker is coupled to the tube through its lower boundary condition where its diaphragm velocity and the air velocity are proportionals:

$$A\widetilde{v}(t, 0) = A_{\mathrm{sp}}\dot{x}_{\mathrm{sp}}(t), \tag{11}$$

where A_{sp} and $x_{\mathrm{sp}}(t)$ are the effective area of the loudspeaker diaphragm and its position, respectively.

Symbols	Values [Units]	Descriptions
ρ_0	1.204 $[Kg\,m^{-3}]$	Air average density
p_0	10^5 $[Pa]$	Air average pressure
T_0	298.15 [K]	Air average temperature
χ_s	$7.04 \cdot 10^{-6}$ $[Pa^{-1}]$	Adiabatic compressibility
c	343 $[m\,s^{-1}]$	Speed of sound

Table 1. Air parameter values

Remark 1. The perturbed wave equation only considers axial plane wave propagations, where transverse waves are rapidly attenuated. For a circular pipe of internal diameter d, the wave equation model is valid below the cutoff frequency $f_c = 1.84118/\pi \times c/d$ (Rossing, 2007, chap. 3), that is in our study case $2.743\ kHz$. Since the measured frequency is $f_0 = 114\,Hz$ and higher harmonics are multiple integers of the natural frequency, this model is valid for the acoustic field.

3.2 Loudspeaker dynamics

We recall here the linear model of loudspeakers (Falaize et al., 2015) illustrated at Figure 2 (left). The two governing equations are derived by applying Kirchhoff's law and Newton's second laws such that:

$$\begin{cases} R_{\mathrm{eff}} I_{\mathrm{sp}}(t) + L_{\mathrm{eff}} \dot{I}_{\mathrm{sp}}(t) + U_L(t) = U_{\mathrm{sp}}(t), \\ m_{\mathrm{eff}}\ddot{x}_{\mathrm{sp}}(t) + d_{\mathrm{eff}}\dot{x}_{\mathrm{sp}}(t) + k_{\mathrm{eff}} x_{\mathrm{sp}}(t) = F_L(t) - F_{\mathrm{d}}(t), \end{cases} \tag{12}$$

where $I_{\mathrm{sp}}(t)$ and $x_{\mathrm{sp}}(t)$ denote the current supplied to the loudspeaker and the diaphragm position, respectively. The inputs of the loudspeaker are the applied voltage $U_{\mathrm{sp}}(t)$

Symbols	Values [Units]	Descriptions
A_{sp}	87 $[cm^2]$	Area
m_{eff}	3.8 $[g]$	Mass
R_{eff}	8.0 $[\Omega]$	Impedance
$(Bl)_{\mathrm{sp}}$	1.7 $[Tm]$	Force factor
f_{sp}	110 $[Hz]$	Resonance frequency
L_{eff}	0.22 $[mH]$	Inductance

Table 2. Loudspeaker's parameter values

and the external force applied to the diaphragm $F_{\mathrm{d}}(t)$. This last force is generated by the acoustic pressure as:

$$A_{\mathrm{sp}} F_{\mathrm{d}}(t) = A\widetilde{p}(t, 0). \tag{13}$$

The counter–electromotive force generated by the coil is labelled $U_L(t) = (Bl)_{\mathrm{sp}} \dot{x}_{\mathrm{sp}}(t)$ and the Lorentz force applied to the diaphragm $F_L(t) = (Bl)_{\mathrm{sp}} I_{\mathrm{sp}}(t)$. The parameter $(Bl)_{\mathrm{sp}}$ denotes the force factor and is the product of the magnetic magnetic inductance field with the coil's length. Furthermore R_{eff} and L_{eff} are the effective loudspeaker resistance and the effective inductance, respectively. The diaphragm mass is labelled m_{eff}. The loudspeaker stiffness k_{eff} is defined as $k_{\mathrm{eff}} = (2\pi f_{\mathrm{sp}})^2 / m_{\mathrm{eff}}$, where f_{sp} is the loudspeaker resonance frequency and the damping coefficient is given by $d_{\mathrm{eff}} = (Bl)^2_{\mathrm{sp}} / R_{\mathrm{eff}}$. All these parameters are reported at Table 2.

Remark 2. Disconnected from a power source the loudspeaker possesses compliance, mass, and damping. When no driving voltage $U_{\mathrm{sp}}(t)$ is applied to the loudspeaker, the resulting boundary dynamics are associated to the disturbance input *i.e.* the acoustic pressure at location $z = 0$.

3.3 Specific acoustic impedance

The specific acoustic impedance at the open top–end of the tube is modelled by a passive RLC circuit (see Figure 2, right). The current $I(t)$ and the voltage $V(t)$ are equivalent to the acoustic velocity $\widetilde{v}(t, l)$ and the acoustic pressure $\widetilde{p}(t, l)$, respectively. Acoustics lumped parameters are defined at Table 3. By applying Kirchhoff's circuit laws one deduces the following state equations:

$$\begin{cases} C_a \dot{V}_C(t) = -I_L(t) - R_{a1}^{-1} V_C(t) + I(t), \\ L_a \dot{I}_L(t) = -R_{a2} I_L(t) + V_C(t) + R_2 I(t), \end{cases} \tag{14}$$

where the input $I(t)$ is equivalent to the acoustic velocity $\widetilde{v}(t, l)$ at the tube edge and the output is the voltage $V(t)$ that is equivalent to the acoustic pressure $\widetilde{p}(t, l)$ defined by:

$$y(t) = -R_{a2} I_L(t) + V_C(t) + R_{a2} I(t), \tag{15}$$

where one remarks the presence of a direct input term $I(t)$ in the output (15).

Symbols	Values [Units]	Descriptions
R_{a1}	$0.504\rho_0 c/A$ $[Pa\,s/m^3]$	Acoustic resistance
R_{a2}	$\rho_0 c/A$ $[Pa\,s/m^3]$	Acoustic resistance
C_a	$5.44a^3/\rho_0 c^2$ $[m^5/N]$	Acoustic capacity
L_a	$0.1952\rho_0/a$ $[kg/m^4]$	Acoustic inductance

Table 3. End impedance acoustic parameters

4. PORT–HAMILTONIAN SUB–SYSTEMS

The Rijke tube model is now derived as a m–phs. It consist of the combination of equations (12), (9), and (14) denoting for the loudspeaker, the disturbed wave equation, and the acoustic open end impedance, respectively. The wave equation (9) is spatially decomposed in two sub–domains $\Omega_1 = [0, z_{\mathrm{h}}]$, and $\Omega_2 = [z_{\mathrm{h}}, l]$, interconnected and coupled at the heating source term location z_{h} with a finite–dimensional nonlinear system modelling the unsteady heat release, a van der Pol oscillator. This spatial decomposition of the dynamics enables us to overcome mathematical problems such as a discontinuity of the solution at point z_{h}, associated with a Dirac distribution $\delta(z - z_{\mathrm{h}})$.

4.1 Acoustic model — two wave equations

In sub–domains Ω_1 and Ω_2 dynamics are governed by two wave equations. Following the modelling of the vibrating string (Jacob and Zwart, 2012) and the vibro–acoustic system (Trenchant et al., 2015), state equations take the form given in (1), where state variables $x_i \in C^2(\Omega_i, \mathbb{R}^2)$, with $i = 1, 2$, are defined as

$$x_i = \begin{bmatrix} x_{i,1}(t, z) \\ x_{i,2}(t, z) \end{bmatrix} = \begin{bmatrix} \overline{\rho}\, \widetilde{v}_i(t, z) \\ \chi_s\, \widetilde{p}_i(t, z) \end{bmatrix}, \tag{16}$$

where $x_{i,1}$, $x_{i,2}$, and $\chi_s = (\gamma \overline{p})$ are the kinetic momentum, the volumetric expansion, and the adiabatic compressibility coefficient, respectively. Structural matrices are equivalent in both domains, where $P_0 = 0$, and P_1 is given by

$$P_1 = \begin{pmatrix} 0 & 1 \\ 1 & 0 \end{pmatrix}. \tag{17}$$

The storage matrix is given as $\mathcal{L} = \operatorname{diag}\left(\overline{\rho}^{-1},\ \chi_s^{-1}\right)$. The associated Hamiltonian function is defined as

$$\mathcal{H}_i(x_i) = \frac{1}{2} \int_{\Omega_i} x_i^\top(t, z) \mathcal{L} x_i(t, z) dz. \tag{18}$$

The Hamiltonian function represents the sum of the kinetic energy and the potential energy. Boundary conditions are defined as a linear combination of the following available boundary port–variables. These are for each sub–domain $\Omega_i = [a, b]$ defined as:

$$\begin{pmatrix} f_{\partial,i} \\ e_{\partial,i} \end{pmatrix} = \frac{1}{\sqrt{2}} \begin{pmatrix} \widetilde{p}_i(b) - \widetilde{p}_i(a) \\ \widetilde{v}_i(b) - \widetilde{v}_i(a) \\ \widetilde{v}_i(b) + \widetilde{v}_i(a) \\ \widetilde{p}_i(b) + \widetilde{p}_i(a) \end{pmatrix}. \tag{19}$$

The first wave equation is defined together with the following boundary condition:

$$u_{\partial\Omega_1} = \begin{pmatrix} \widetilde{v}_1(0) \\ \widetilde{v}_1(z_{\mathrm{h}}) \end{pmatrix} = \begin{pmatrix} W_{B_1,1} \\ W_{B_2,1} \end{pmatrix} \begin{pmatrix} f_{\partial,1} \\ e_{\partial,1} \end{pmatrix} \tag{20}$$

where one used equation (19) to identify the linear applications $W_{B_1,1}$ and $W_{B_2,1}$.The output is

$$y_{\partial\Omega_1} = \begin{pmatrix} -\widetilde{p}_1(0) \\ \widetilde{p}_1(z_{\mathrm{h}}) \end{pmatrix} = \begin{pmatrix} W_{C_1,1} \\ W_{C_2,1} \end{pmatrix} \begin{pmatrix} f_{\partial,1} \\ e_{\partial,1} \end{pmatrix}. \tag{21}$$

The second wave equations has the following input

$$u_{\partial\Omega_2} = \begin{pmatrix} \widetilde{p}_2(l) \\ \widetilde{p}_2(z_{\mathrm{h}}) \end{pmatrix} = \begin{pmatrix} W_{B_1,2} \\ W_{B_2,2} \end{pmatrix} \begin{pmatrix} f_{\partial,2} \\ e_{\partial,2} \end{pmatrix}. \tag{22}$$

Outputs of the second wave equation are set as:

$$y_{\partial\Omega_2} = \begin{pmatrix} \widetilde{v}_2(l) \\ \widetilde{v}_2(z_{\mathrm{h}}) \end{pmatrix} = \begin{pmatrix} W_{C_1,2} \\ W_{C_2,2} \end{pmatrix} \begin{pmatrix} f_{\partial,2} \\ e_{\partial,2} \end{pmatrix}. \tag{23}$$

Interconnection of the wave equations is detailed in paragraph (5.1). With the defined input/output pairs, both wave equations are independently well-posed, see (Jacob and Zwart, 2012, Theorem 13.2.2).

4.2 Loudspeaker

The loudspeaker state variables are the induced magnetic flux $\phi(t) = L_{\mathrm{eff}} I_{\mathrm{sp}}(t)$, the diaphragm position $x_{\mathrm{sp}}(t)$, and the diaphragm momentum $m_{\mathrm{eff}} \dot{x}_{\mathrm{sp}}(t)$ such that the state vector $X_{\mathrm{sp}}(t) \in \mathbb{R}^{3\times 1}$ is defined as:

$$X_{\mathrm{sp}}(t) = \left[\phi(t),\ x_{\mathrm{sp}}(t),\ m_{\mathrm{eff}} \dot{x}_{\mathrm{sp}}(t)\right]^\top. \tag{24}$$

The storage Hamiltonian function of the loudspeaker is given by the following quadratic function:

$$H\left(X_{\rm sp}\right) = \frac{1}{2} X_{\rm sp}^{\top}(t) G_{\rm sp} X_{\rm sp}(t), \tag{25}$$

that is the sum of the kinetic energy, the potential energy, and the magnetic energy. The storage matrix $G_{\rm sp} = \operatorname{diag}\left(L_{\rm eff}^{-1},\, k_{\rm eff},\, m_{\rm eff}^{-1}\right) = G_{\rm sp}^{\top} \in M_3\left(\mathbb{R}\right)$ is a positive–definite matrix.

The loudspeaker dynamics are re–formulated within the following port–Hamiltonian form:

$$\begin{cases} \dot{X}_{\rm sp}(t) = \left[J_{\rm sp} - R_{\rm sp}\right] G_{\rm sp} X_{\rm sp}(t) + g_{\rm sp} u_{\rm sp}(t), \\ y_{\rm sp}(t) = g_{\rm sp}^{\top} G_{\rm sp} X_{\rm sp}(t). \end{cases} \tag{26}$$

The interconnection matrix $J_{\rm sp} = -J_{\rm sp}^{\top} \in M_3\left(\mathbb{R}\right)$ defined as :

$$J_{\rm sp} = \begin{pmatrix} 0 & 0 & -(Bl)_{\rm sp} \\ 0 & 0 & 1 \\ (Bl)_{\rm sp} & -1 & 0 \end{pmatrix}.$$

The dissipative matrix $R_{\rm sp} = \operatorname{diag}\left(R_{\rm eff},\, 0,\, d_{\rm eff}\right) = R_{\rm sp}^{\top} \in M_3\left(\mathbb{R}\right)$ is positive semi–definite. The input matrix $g_{\rm sp} \in M_{2\times 3}(\mathbb{R})$ is given by

$$g_{\rm sp}^{\top} = \begin{pmatrix} 1 & 0 & 0 \\ 0 & 0 & 1 \end{pmatrix}.$$

The two inputs are the voltage applied to the loudspeaker and the force applied by acoustic pressure on the loudspeaker diaphragm, as $u_{\rm sp}^{\top}(t) = \left[U_{\rm sp}(t),\, -F_d(t)\right]$. Furthermore the two outputs are the loudspeaker current and the velocity of the diaphragm such that $y_{\rm sp}^{\top}(t) = \left[I_{\rm sp}(t),\, \dot{x}_{\rm sp}(t)\right]$.

Remark 3. To increase the compliance of the model one may consider to include the possible nonlinearities. Indeed the diaphragm stiffness saturation property fits within the port–Hamiltonian formulation (Falaize et al., 2015).

4.3 Boundary Layer Model – van der Pol Oscillator

The time varying heat release term is modelled by a van der Pol oscillator, where the boundary layer displacement $\xi_1(t) \in \mathbb{R}$ and velocity $\xi_2(t) \in \mathbb{R}$ dynamics are governed by the following nonlinear ordinary differential equation:

$$\begin{cases} \begin{pmatrix} \dot{\xi}_1 \\ \dot{\xi}_2 \end{pmatrix} = \begin{pmatrix} 0 & 1 \\ -1 & r_{22}(\xi_1) \end{pmatrix} \begin{pmatrix} \omega_0^2 & 0 \\ 0 & 1 \end{pmatrix} \begin{pmatrix} \xi_1 \\ \xi_2 \end{pmatrix} + \begin{pmatrix} 0 \\ B_{\rm h} \end{pmatrix} u_{\rm h}, \\ y_{\rm h} = B_{\rm h} \xi_2 \end{cases} \tag{27}$$

where $\omega_0 = 2\pi f_0$ denotes for the natural tube pulsation and $u_{\rm h}(t)$ represents the boundary layer velocity. The nonlinear element $r_{22}(\xi_1) = \varepsilon\left(1 - \mu\xi_1^2\right)$, where ξ_1, where parameters ε and μ are positive real values, changes sign.

Property 1. The sign of $r_{22}(\xi_1)$ is function of ξ_1:

- $\forall \xi_2 \in \mathbb{R},\, |\xi_1| \leq \mu^{-1}$ then $r_{22}(\xi_1) \leq 0$
- $\forall \xi_2 \in \mathbb{R},\, |\xi_1| > \mu^{-1}$, then $r_{22}(\xi_1) > 0$.

In the first case r_{22} represents a damping term, while in the second case it is a forcing term.

The total energy of the van der Pol oscillator (27) is given as

$$H_{\rm vdp}(\xi_1, \xi_2) = \frac{1}{2}\omega_0^2 \xi_1^2 + \frac{1}{2}\xi_2^2, \tag{28}$$

with time derivative given by

$$\dot{H}_{\rm vdp}\left(\xi_1, \xi_2\right) = r_{22}(\xi_1)\xi_2^2 + u_{\rm h} y_{\rm h}. \tag{29}$$

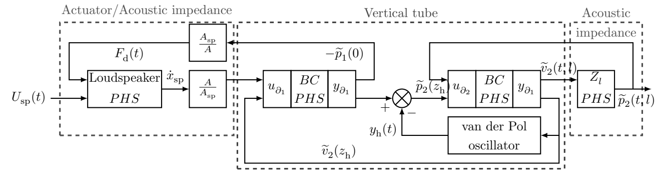

Fig. 3. Rijke's tube block diagram

This leads to the following property of the van der Pol oscillator.

Lemma 1. The system (27) is passive with the storage function $E(\xi_1, \xi_2)$ if and only if $|\xi_1| \leq \mu^{-1}$.

4.4 Specific acoustic impedance

We recast here the specific acoustic impedance model defined by the state equations (14). We consider as state variables $X_{\rm a}(t) = \left[L_a I_L(t),\, C_a V_C(t)\right]^{\top}$ the flux and charge in the circuit, respectively. The input $u_{\rm a}(t)$ is defined as the current $I_(t)$, that is the acoustic velocity at location $z = l$. A quadratic Hamiltonian function is considered, such that:

$$H_{\rm a}(X_{\rm a}) = \frac{1}{2} X_{\rm a}^{\top}(t) G_{\rm a} X_{\rm a}(t), \tag{30}$$

where $G_{\rm a} = \operatorname{diag}\left(L_a^{-1},\, C_a^{-1}\right) \in M_2(\mathbb{R})$ is the storage matrix. The governing equations are now expressed as:

$$\begin{cases} \dot{X}_{\rm a}(t) = \left[J_{\rm a} - R_{\rm a}\right] G_{\rm a} X_{\rm a}(t) + \left[g_{\rm a} - S_{\rm a}\right] u_a(t), \\ y(t) = \left[g_{\rm a}^{\top} + S_{\rm a}^{\top}\right] G_{\rm a} X_{\rm a}(t) + R_{a2} u_a(t), \end{cases} \tag{31}$$

where the conservative and the dissipative matrices are defined as follows:

$$J_{\rm a} = \begin{pmatrix} 0 & 1 \\ -1 & 0 \end{pmatrix} = -J_{\rm a}^{\top} \in M_2(\mathbb{R})$$

and $R_{\rm a} = \operatorname{diag}\left(R_{a2},\, R_{a1}^{-1}\right) = R_{\rm a}^{\top} \in M_2(\mathbb{R})$. The inputs matrices are $g_{\rm a}^{\top} = (0,\, 1)$ and $S_{\rm a}^{\top} = (-R_{a2},\, 0)$.

5. MIXED CONTROL MODEL

The Rijke tube model is governed, from bottom to top, by the interconnection of the loudspeaker (26), the two wave equations (1) with boundary conditions (20)–(23), the van der Pol oscillator (27), and the acoustic impedance (31). The interconnected system is depicted at Figure 3. The global model possesses the following state vector:

$$\widetilde{x} = \left[x_1,\, x_2,\, \xi_1,\, \xi_2,\, \phi,\, x_{\rm sp},\, m_{\rm sp}\dot{x}_{\rm sp},\, C_{\rm a} V_C,\, L_{\rm a} I_L\right]^{\top},$$

defined in a state space being the Cartesian product of all sub–space' state spaces, where an inner product and a norm are defined.

5.1 Couplings

The loudspeaker and the wave equation in domain Ω_1 are linked through the power–preserving interconnection (11) and (13). The first and the second wave equations are interconnected at the heating point $z = z_{\rm h}$ and coupled to the heating element through the following power–preserving interconnection

$$\begin{cases} \widetilde{v}_1(t, z_{\rm h}) = \widetilde{v}_2(t, z_{\rm h}), \\ \widetilde{p}_1(t, z_{\rm h}) = \widetilde{p}_2(t, z_{\rm h}) + y_{\rm h}(t). \end{cases} \tag{32}$$

Furthermore at the tube open top–end the $u_{\rm a}(t) = \widetilde{v}_2(t, l)$ and $y_{\rm a}(t) = \widetilde{p}_2(t, l)$.

5.2 Total Hamiltonian function

The total Hamiltonian function $H_{\text{tot}}(t) \in \mathbb{R}$ is given by the sum of all sub–systems Hamiltonian function as:

$$H_{\text{tot}}(\widetilde{x}) = H_{\text{sp}} + H_{\text{vdp}} + \sum_{i=1}^{2} \mathcal{H}_i + H_{\text{a}}. \tag{33}$$

The time derivative of the total Hamiltonian function depends one the nonlinear term $r_{22}(\xi_2)$, as in (29), that breaks the passivity property of the complete system.

Remark 4. Note that the van der Pol oscillator is interconnected with the second wave equations in a similar manner than carried out in (Ramírez et al., 2017). A major difference being that the nonlinear coefficient $r_{22}(\xi_2)$ breaks the dissipative property. The development of structured control laws for this application remains to be achieved.

5.3 Limits of the mixed port–Hamiltonian model

As defined, the open loop model of the Rijke tube has weaknesses. First of all the van der Pol oscillator representing the boundary layer dynamics is not a first–principle model and do not explains thermo–acoustic instabilities. Furthermore the non passivity property of the oscillator prevents the use of classical port–Hamiltonian control techniques.

Remark 5. The model introduced here is closely related to the one studied in Ramírez et al. (2017) where the nonlinear lumped system is assumed to be passive. If one decides to use the van der Pol oscillator this assumption has to be relaxed.

6. CONCLUSIONS AND FUTURE WORKS

The paper is devoted to the m–phs representation of thermo–acoustics instabilities. Limits of this model are highlight: the lack of physics–based representation for the boundary layer and the expected control issues with the van der Pol model.

Future works include a thermodynamically–based modelling of the boundary layer, and an early lumping structured control based on geometric discretization (Cardoso-Ribeiro et al., 2017) with expected experimental validations.

REFERENCES

Annaswamy, A.M. and Ghoniem, A.F. (2002). Active control of combustion instability: theory and practice. *IEEE Control Systems Magazine*, 22(6), 37–54.

Cardoso–Ribeiro, F., Matignon, D., and Pommier–Budinger, V. (2017). A port–Hamiltonian model of liquid sloshing in moving containers and application to a fluid–structure system. *Journal of Fluids and Structures*, 69, 402–427.

Chu, Y.C., Glover, K., and Dowling, A.P. (2003). Control of combustion oscillations via h_∞ loop–shaping, μ–analysis and integral quadratic constraints. *Automatica*, 39(2), 219–231.

Culick, F.E. and Kuentzmann, P. (2006). Unsteady motions in combustion chambers for propulsion systems. Technical report, NATO research and technology organization Neilly–sur–Seine, France.

de Andrade, G.A., Vazquez, R., and Pagano, D.J. (2018a). Backstepping stabilization of a linearized ODE-–PDE Rijke tube model. *Automatica*, 96, 98–109.

de Andrade, G., Vazquez, R., and Pagano, D. (2018b). Backstepping–based linear boundary observer for estimation of thermoacoustic instabilities in a Rijke tube. In *57th IEEE, CDC 2018, Miami, FL, USA, December 17–19, 2018*, 2164–2169.

Dowling, A.P. and Morgans, A.S. (2005). Feedback control of combustion oscillations. *Annu. Rev. Fluid Mech.*, 37, 151–182.

Duindam, V., Macchelli, A., Stramigioli, S., and Bruyninckx, H. (2009). *Modeling and Control of Complex Physical Systems: The Port-Hamiltonian Approach.* Springer, Berlin Heidelberg.

Epperlein, J., Bamieh, B., and Astrom, K. (2015). Thermoacoustics and the Rijke tube: Experiments, identification, and modeling. *IEEE Control Systems*, 35(2), 57–77.

Falaize, A., Papazoglou, N., Hélie, T., and Lopes, N. (2015). Compensation of loudspeaker's nonlinearities based on flatness and port–Hamiltonian approach. In *22ème Congrès Français de Mécanique.*

Fung, Y.T. and Yang, V. (1992). Active control of nonlinear pressure oscillations in combustion chambers. *Journal of Propulsion and Power*, 8(6), 1282–1289.

Heckl, M.A. (1988). Active control of the noise from a Rijke tube. *Journal of Sound and Vibration*, 124(1), 117–133.

Jacob, B. and Zwart, H. (2012). *Linear port–Hamiltonian systems on infinite–dimensional spaces.* Springer.

Jacobson, C., Khibnik, A., Banaszuk, A., Cohen, J., and Proscia, W. (2000). Active control of combustion instabilities in gas turbine engines for low emissions. Part I: Physics–based and experimentally identified models of combustion instability. Technical report, United Technologies Research Center East Hartford, CT.

Krstic, M., Krupadanam, A., and Jacobson, C. (1999). Self–tuning control of a nonlinear model of combustion instabilities. *IEEE Transactions on Control Systems Technology*, 7(4), 424–436.

Noiray, N. and Schuermans, B. (2013). Deterministic quantities characterizing noise driven Hopf bifurcations in gas turbine combustors. *International Journal of Non-Linear Mechanics*, 50, 152–163.

Ramírez, H., Zwart, H., and Le Gorrec, Y. (2017). Stabilization of infinite dimensional port–Hamiltonian systems by nonlinear dynamic boundary control. *Automatica*, 85, 61–69.

Rayleigh, J.W.S. (1878). The explanation of certain acoustical phenomena. *Nature*, 319–321.

Rossing, T. (2007). *Springer Handbook of Acoustics.* Springer Science & Business Media.

Trenchant, V., Fares, Y., Ramírez, H., and Le Gorrec, Y. (2015). A port–Hamiltonian formulation of a 2D boundary controlled acoustic system. *IFAC-PapersOnLine*, 48(13), 235 – 240. 5th IFAC Workshop on Lagrangian and Hamiltonian Methods for Nonlinear Control LHMNC 2015.

Zimmer, B.J., Lipshitz, S.P., Morris, K., Vanderkooy, J., and Obasi, E.E. (2003). An improved acoustic model for active noise control in a duct. *Journal of dynamic systems, measurement, and control*, 125(3), 382–395.